PERGAMON

Deep-Sea Research II 49 (2002) 3655–3674

DEEP-SEA RESEARCH
PART II

www.elsevier.com/locate/dsr2

Upwelling intensity and filament activity off Morocco during the last 250,000 years

Tim Freudenthal[a,*], Helge Meggers[a], Jorijntje Henderiks[b], Holger Kuhlmann[a], Ana Moreno[c], Gerold Wefer[a]

[a] *Universität Bremen, Geowissenschaften, Postfach 330440, D-28334 Bremen, Germany*
[b] *ETH-Z, Geologisches Institut, Sonneggstrasse 5, CH-8092 Zürich, Switzerland*
[c] *Facultat de Geologia, Universitat de Barcelona, c/Martí i Franquès, s/n, 08028 Barcelona, Spain*

Received 19 April 2000; received in revised form 29 November 2000; accepted 19 February 2001

Abstract

The high-productive upwelling area off Morocco is part of one of the four major trade-wind driven continental margin upwelling zones in the world oceans. While coastal upwelling occurs mostly on the shelf, biogenic particles derived from upwelling are deposited mostly at the upper continental slope. Nutrient-rich coastal water is transported within the Cape Ghir filament region at 30°N up to several hundreds of kilometers offshore. Both upwelling intensity and filament activity are dependent on the strength of the summer Trades. This study is aimed to reconstruct changes in trade wind intensity over the last 250,000 years by the analysis of the productivity signal contained in the sedimentary biogenic particles of the continental slope and beneath the Cape Ghir filament. Detailed geochemical and geophysical analyses (TOC, carbonate, C/N, $\delta^{13}C_{org}$, $\delta^{15}N$, $\delta^{13}C$ of benthic foraminifera, $\delta^{18}O$ of benthic and planktic foraminifera, magnetic susceptibility) have been carried out at two sites on the upper continental slope and one site located further offshore influenced by the Cape Ghir filament. A second offshore site south of the filament was analyzed (TOC, magnetic susceptibility) to distinguish the productivity signal related to the filament signal from the general offshore variability. Higher productivity during glacial times was observed at all four sites. However, the variability of productivity during glacial times was remarkably different at the filament-influenced site compared to the upwelling-influenced continental slope sites. In addition to climate-related changes in upwelling intensity, zonal shifts of the upwelling area due to sea-level changes have impacted the sedimentary productivity record, especially at the continental slope sites. By comparison with other proxies related to the strength and direction of the prevailing winds (Si/Al ratio as grain-size indicator, pollen) the productivity record at the filament-influenced site reflects mainly changes in trade-wind intensity. Our reconstruction reveals that especially during glacial times trade-wind intensity was increased and showed a strong variability with frequencies related to precession. © 2002 Elsevier Science Ltd. All rights reserved.

1. Introduction

Near-shore upwelling of nutrient-enriched sub-thermocline waters and their offshore transport in eddies and filaments result in high rates of primary production and fixation of carbon. Upwelling

*Corresponding author. Tel.: +49-421-2187760; fax: +49-421-2183116.
E-mail address: freuden@allgeo.uni-bremen.de (T. Freudenthal).

PII: S0967-0645(02)00101-7

regions thus play an important role in global carbon cycling. Changes in upwelling intensity and consequent changes in primary productivity have been proposed to explain part of the changes of climate-sensitive atmospheric CO_2 concentrations on glacial–interglacial time-scales (Sarnthein et al., 1987). Both upwelling intensity and the formation and extension of filaments (in the following named filament activity) are dependent on regional climate, especially on the strength and duration of along-shore winds (Speth et al., 1978; Lutjeharms and Meeuwis, 1987; McCreary et al., 1991; Strub et al., 1991; Nykjær and Van Camp, 1994). Thus, detection of past productivity variations in upwelling regions can be used to infer changes in past wind circulation (Müller et al., 1983; Hughen et al., 1996).

A variety of micropaleontological and geochemical methods have been developed to reconstruct past variations in export production and variations in water mass characteristics that depend on upwelling intensity, like sea-surface temperature, salinity, or nutrient availability. A comprehensive overview about the use of these methods in paleoceanography has been given by Wefer et al. (1999).

The influence of sea-level changes on the sedimentary productivity record only recently has been discussed and is poorly understood (Guichard et al., 1999; Martinez et al., 1999; Bertrand et al., 2000). During the last glacial maximum (LGM) sea-level was about 120 m lower compared to present-day conditions (Fairbanks, 1989). At present, upwelling occurs mostly on the shelf (Mittelstaedt, 1991). A retreat of the coastline towards the edge of the shelf during times of low sea-level forces an offshore movement of the upwelling center towards the continental slope. Thus, changes in the sedimentary productivity record might be induced by changes in the upwelling intensity and/or by changes in the distance of the investigation site to the upwelling center. Additionally, lateral particle transport and nutrient dynamics may have changed during times of low sea level compared to present conditions (Fütterer, 1983; Bertrand et al., 2000). Using sedimentary paleoproductivity records as paleoclimatic archives can be facilitated by separating the impact of sea-level changes from wind-induced changes in upwelling intensity. This is hardly achievable, however, when only one site is assumed to be representative for the entire upwelling system, as done in most previous studies.

In this study we use geochemical methods to show how productivity variations over the last 250,000 years are preserved in marine sediments off Morocco (NW Africa). We try to distinguish between the influence of sea-level change and variations in trade-wind intensity on the sedimentary paleoproductivity record, by investigating four different sites (Fig. 1). Two sites are located at the continental slope near the coastal upwelling area. The other two sites are located further offshore, one off Cape Ghir, a region of intensive present-day filament activity. We show that the climatic signal is strongly overprinted by the impact of sea-level variations at the upwelling-influenced coastal sites. The filament-influenced site is highly sensitive to climatic-induced changes in productivity during glacial times. The summer NE trade-wind circulation that controls upwelling activity and filament intensity off Morocco, seems to be strongly controlled by precessional forcing mechanisms.

2. Present-day climate and oceanography off NW Africa

The NE trade-wind belt is the prevailing wind system off NW Africa. Seasonal variations are caused by the latitudinal shift of the subtropical high-pressure system currently known as the Azores High and of the tropical deep-pressure system related to the Inter-Tropical Convergence Zone. During the boreal winter, the trade-wind belt is mainly located between 10°N and 25°N. During boreal summer, trade winds blow prevalently between 20°N and 32°N.

The main direction of the trade winds along the NW African coast is along-shore, thus generating upwelling of cold and nutrient-rich waters along this coast by Ekman transport and coastal eddies. According to the seasonal migration of the trade-wind belt, summer and fall are the seasons of

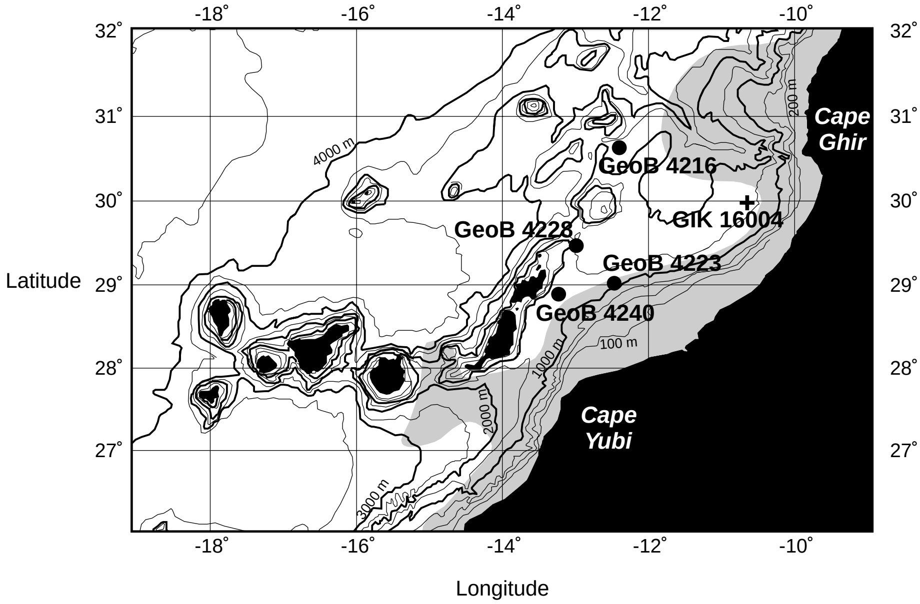

Fig. 1. Bathymetric map showing the investigation area off Morocco. Circles indicate the position of sites investigated in this study. A further site discussed in this study (GIK 16004) is marked by a cross. The main area of higher pigment concentrations related to coastal upwelling and the Cape Ghir filament, based on an 18-day stack of SeaWiFS images in 1998 (Freudenthal et al., 2002), is shaded.

strongest upwelling off Morocco. Upwelling is observed in a coastal band about 50 km wide, mainly on the continental shelf (Van Camp et al., 1991). The shelf has a width of 30–100 km. Water depth on the shelf is mainly below 100 m (Fig. 1).

The main current off NW Africa is the southward-directed Canary Current that is associated with the coastal upwelling (Mittelstaedt, 1991). The interaction of the Canary Current, coastal upwelling, and morphological features of coast and continental shelf leads to the development of meanders that carry cold and nutrient-rich coastal waters in filament form into the warm subtropical gyre region (Johnson and Stevens, 2000). One of the most prominent areas of filament activity off Morocco is located west of Cape Ghir and reaches occasionally several hundred kilometers offshore (Van Camp et al., 1991; Nykjær and Van Camp, 1994; Hagen et al., 1996). The filament activity is similar to coastal upwelling dependent on the strength and duration of the trade winds, although a 3-month phase lag has been observed between the onset of the maximum trade winds in summer and the time of most intense upwelling off Cape Ghir (Nykjær and Van Camp, 1994). High pigment concentrations indicating high productivity are observed both in filaments and the coastal upwelling zone (Van Camp et al., 1991; Davenport et al., 1999; Freudenthal et al., 2001a) (Fig. 1).

The preservation of the productivity signal in the sediments is largely dependent on the bottom-water-mass characteristics, especially oxygen concentration. The water-mass stratification and oxygenation off NW Africa was reviewed by Sarnthein et al. (1982) and Siedler and Onken (1996). Below the Subtropical water, the North Atlantic Central Water (100–600 m), the Mediterranean Outflow Water (MOW, centered at about 1200 m), and the North Atlantic Deep Water (NADW, below 2000 m) are the characteristic water masses in the investigation area. In some cases an influence of a derivative of Antarctic Intermediate Water (500–1000 m) was observed north of the Canary Islands that was carried above the continental slope by the pole ward undercurrent (Mittelstaedt, 1991; Müller et al., 1999; Knoll et al., 2002). All water masses are well oxygenated at present day conditions.

Table 1
Location, water depth, and length of investigated gravity and piston cores

Site	Device	Latitude (°N)	Longitude (°W)	Water depth (m)	Core recovery (cm)
GeoB 4216	Gravity corer	30°38	12°24	2324	1117
GeoB 4223	Gravity corer	29°01	12°28	775	779
GeoB 4228	Piston corer	29°29	12°59	1638	1188
GeoB 4240	Gravity corer	28°53	13°14	1358	688

3. Materials and methods

The four sediment cores investigated in this study were recovered during Meteor cruise M37/1 in December 1996 (Wefer et al., 1997). Two sites were located at the continental slope (GeoB 4223, GeoB 4240), and two farther offshore (GeoB 4216, GeoB 4228) (Fig. 1; Table 1). Upwelling occurs mostly on the shelf. However, most biogenic fluxes derived from the upwelling are deposited at the continental slope between 1000 and 1500 m, due to remobilization and transport across the shelf (Fütterer, 1983). Therefore, we consider the continental slope sites as upwelling-influenced sites. Site GeoB 4216 is located west of Cape Ghir and may thus be influenced by high-productivity conditions related to the Cape Ghir filament. In present-day situations the offshore extension of the filament region only occasionally influences this site. While a clear imprint of increased productivity was observed in the underlying surface sediments east of our study site, the productivity record at the sediment surface of site GeoB 4216 is typical for the oligotrophic offshore region (Meggers et al., 2002). However, we expect a significant impact during times of increased trade winds and stronger filament activity in the past. We selected site GeoB 4228 as offshore reference site for comparison with site GeoB 4216 in order to be able to distinguish the productivity signal related to the Cape Ghir filament and the offshore "background" signal of productivity variations.

3.1. Core descriptions

Opening and visual description of the sediment cores was conducted on board the ship (Fischer et al., 1997; Wefer et al., 1997), except for core GeoB 4240, which was opened at the University of Bremen. Sediments consist mainly of light brownish or olive green undisturbed nannofossil ooze. At cores GeoB 4216 and GeoB 4228 a volcanic ash layer was identified at 768 and 693 cm sediment depth, respectively. A second ash layer was identified at 1098 cm sediment depth in core GeoB 4216 and at 997 cm sediment depth in core GeoB 4228. The ash-layers were used for stratigraphic correlation of cores GeoB 4216 and GeoB 4228. Two sand layers containing biogenic coarse-grained carbonates at about 160 and 485 cm sediment depth of 4.5 and 3 cm thickness, respectively, were observed in core GeoB 4228. We interpret them as turbidites. At core GeoB 4240 three sand layers of 1–1.5 cm thickness containing volcanic material were observed at 172, 178, and 182 cm sediment depth.

3.2. Geophysical and geochemical properties

Magnetic susceptibility was measured in 1-cm steps using a GEOTEK Multi Sensor Core Logger. Geochemical analysis was conducted with a sample spacing of 5 cm. Analyses of TOC, carbonate, C/N, $\delta^{15}N$, and $\delta^{13}C_{org}$ were conducted on freeze-dried and homogenized sediment samples. For the measurement of carbon concentrations, samples were placed in ceramic crucibles and analyzed using a LECO CS-244 determinator. TOC was measured after treatment of sediment with 6 M HCl and heating at 80°C. A small loss of acid-soluble organic carbon through the walls of the crucibles (<0.1 wt%) was negligible compared to the observed variability of TOC concentrations. Carbonate concentrations were calculated from the total carbon (TC) content, measured on untreated samples as $CaCO_3 = (TC - TOC) \times$

8.333. We calculated TOC and carbonate concentrations on salt-free basis, using wet-weight and dry-weight determinations for calculation of pore-water content and assuming a salinity of 35‰. Precision of TOC and carbonate analysis was better than 3% and 2%, respectively.

For the analysis of C/N ratio, $\delta^{15}N$, and $\delta^{13}C_{org}$ samples were placed in tin boats and combusted at 1050°C in an NC 2500 Elemental Analyzer (CE Instruments). The $\delta^{15}N$ and $\delta^{13}C$ of the gas thus formed was measured using a Finnigan MAT delta plus mass spectrometer. The ratio of ^{12}C to ^{14}N was used for calculation of the C/N ratio after calibration against a laboratory sediment standard. The $\delta^{15}N$ of sediments from cores GeoB 4223 and GeoB 4240 was measured on untreated sediment samples. Due to the low nitrogen concentrations at large parts of core GeoB 4216, we determined $\delta^{15}N$ at this site after decalcifying with 1 M HCl and washing with deionized water. The $\delta^{15}N$ of decalcified samples correlated well with $\delta^{15}N$ of untreated samples at sites GeoB 4223 and GeoB 4240 ($r^2 = 0.75$; $n = 286$) with decalcified samples, being on average 0.11‰ lighter compared to untreated samples. $\delta^{13}C_{org}$ and C/N ratios were measured on decalcified samples.

The stable oxygen ($\delta^{18}O$) and carbon ($\delta^{13}C$) isotope ratios of benthic and planktic foraminifera were analyzed using a Finnigan MAT 251 mass spectrometer with an automated carbonate preparation device at the University of Bremen. Each measurement was performed on 10–15 individual shells of the planktic foraminifer *Globigerina bulloides* (200–250 μm) and 3–6 shells of the epibenthic foraminifer *Cibicidoides wuellerstorfi* at sites GeoB 4216 and GeoB 4240. Due to the low abundance of *C. wuellerstorfi*, we used the endobenthic foraminifer *Uvigerina peregrina* at site GeoB 4223. The isotopic composition of the shells was measured on the CO_2 gas released after treatment of the shells with phosphoric acid at a constant temperature of 75°C.

For all stable oxygen and carbon isotope measurements we used a working standard (Burgbrohl CO_2 gas), which has been calibrated with NBS 18, 19, and 20 standards against PDB. For the stable nitrogen isotope measurements 99.996% pure tank N_2 was used as working standard. It was calibrated against air using IAEA standards N-1 and N-2. Analytical standard deviation is about ±0.05‰ for $\delta^{13}C$ and ±0.07‰ for $\delta^{18}O$ of carbonate shells. Precision calculated from repeated measurements on a laboratory sediment standard was about ±0.1‰ for $\delta^{13}C_{org}$, ±0.2‰ for $\delta^{15}N$, and ±0.5 for the C/N ratio.

The geophysical and geochemical parameters were completely analyzed at the upwelling-influenced sites GeoB 4223 and GeoB 4240 and at the filament-influenced site GeoB 4216. For the analysis of the offshore organic background sedimentation at site GeoB 4228 we focussed on the analysis of TOC and on magnetic susceptibility for stratigraphic comparison.

4. Results

4.1. Stratigraphy

Age control at sites GeoB 4216, GeoB 4223, and GeoB 4240 was obtained by correlating the $\delta^{18}O$ records with the SPECMAP stack (Imbrie et al., 1984) (Fig. 2). For this purpose the planktic $\delta^{18}O$ records were used, since they have been measured with high resolution at all three sites using the same species (*G. bulloides*). In our study, the major transitions, stadials, and interstadials could be easily identified in all three cores, besides oxygen isotope event 3.0. For oxygen isotope event 2.0 we assumed an age of 13.5 ka (Raymo, 1997). More detailed time control of the events surrounding the last Termination was obtained by correlating planktic $\delta^{18}O$ records of the upper parts of the three cores with the planktic $\delta^{18}O$ record from core SU81-18, which has been dated by ^{14}C-AMS in great detail and is located north of our investigation area off Portugal (Bard et al., 1989). We converted the ^{14}C ages into calendar ages using the program CALIB 4.1 (Stuiver and Braziunas, 1993) and the INTCAL98 data set for marine carbonates (Stuiver et al., 1998). Ages between the tie points were obtained by linear interpolation.

Strong time coherence in the variability of magnetic susceptibility is recognized at all three sites when applying the age models to the magnetic

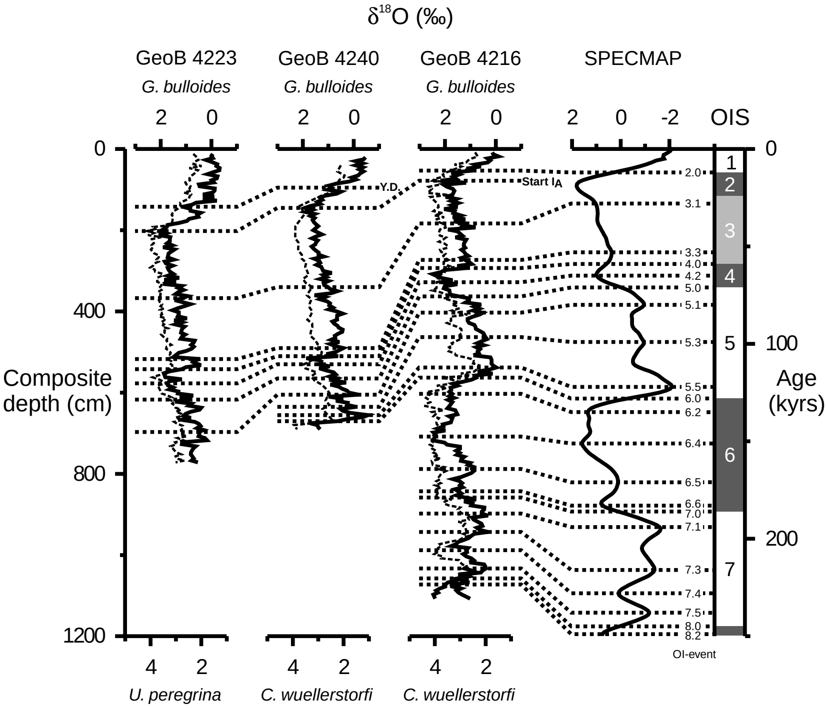

Fig. 2. Depth records of planktic (bold line) and benthic (thin line) oxygen isotope ratios of cores GeoB 4223, GeoB 4240 and GeoB 4216 compared to the SPECMAP stack (Imbrie et al., 1984). Composite depth includes core depth and estimated sediment loss during coring (5–17 cm, (Henderiks et al., 2002). Correlation of the planktic records with the SPECMAP stack is indicated by dotted lines. In addition, events during the last termination used as tie points are indicated (Y.D.: Younger Dryas; Start I_A: Start of Termination I). The right bar indicate oxygen isotope stages (OIS), with glacial stages in dark gray and interglacial stages in white. Although OIS 3 is an interglacial stage per definition, it is shaded in light gray, due to its strong glacial climatic character (compare Sarnthein et al., 1987).

susceptibility records in cores GeoB 4216, GeoB 4223, and GeoB 4240 (Fig. 3). Age control of GeoB 4228, where no oxygen isotope data are available, was obtained by correlating magnetic susceptibility with the age-dated magnetic susceptibility profile of core GeoB 4216.

Several ^{14}C measurements on *G. bulloides* and on mixed planktic foraminifera samples of cores GeoB 4223 and GeoB 4240 (Henderiks et al., 2002) support our age models (Fig. 4a). However, three samples around the oxygen isotope event 3.1 yielded different results: While one measurement on *G. bulloides* agreed with our age model, two mixed samples were about 4 ka older. The reason for the strong differences in the ^{14}C ages of monospecific and mixed samples is not clear (see for discussion Henderiks et al., 2002).

Higher average sedimentation rates were observed at the near-coastal sites GeoB 4223 and GeoB 4240 (average 8.7 and 5.2 cm/ka, respectively) compared to the open-ocean sites GeoB 4216 and GeoB 4228 (average 4.3 and 4.0 cm/ka, respectively) (Fig. 4a and b). Sedimentation rates were higher during glacial times than during interglacial times at all four sites. Unusual sedimentation rates below 2 cm/ka during oxygen isotope stage (OIS) 5 at site GeoB 4240 may be explained by sediment winnowing during the last interglacial.

4.2. Geochemical results at the offshore sites GeoB 4216 (filament influenced) and GeoB 4228 (not influenced)

The records of different geochemical proxies related to productivity at the Cape Ghir filament influenced site GeoB 4216 are shown in Fig. 5. TOC concentrations are generally low (mostly

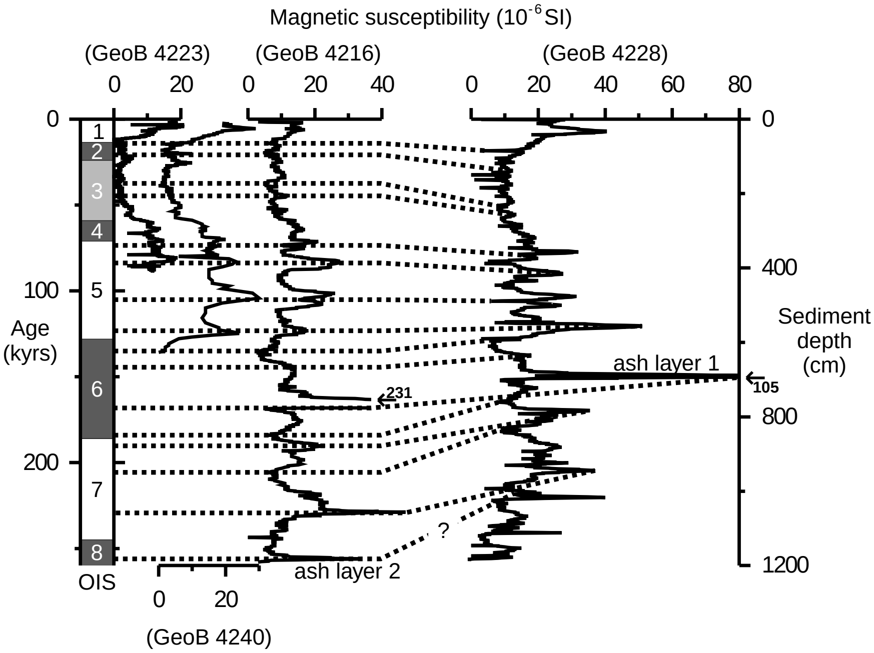

Fig. 3. Magnetic susceptibility of core GeoB 4228 and correlation with magnetic susceptibility of cores GeoB 4216, GeoB 4223, and GeoB 4240. Numbers at arrows indicate maximal magnetic susceptibility at ash layer 1 that was used for stratigraphic correlation.

<0.2%) during interglacial OISs 1, 5, and 7. During glacial OISs 2, 3, 4, 6, and 8 concentrations are generally higher (0.2–0.8%) and show a strong variability. Distinct TOC peaks named P1–P10 were observed at 15 (Termination I), 24, 32, 43, 63, 128 (Termination II), 152, 178, 224 (substadial 7.4), and 242 (Termination III) ka BP (Fig. 5). While Terminations I+II are characterized by strongest TOC peaks, the peak at Termination III is much less pronounced. Site GeoB 4228 as a reference site for offshore conditions with less influence of the Cape Ghir filament, shows similar to site GeoB 4216 higher TOC concentrations during glacial times (Fig. 5). However, with the exception of a distinct peak during Termination II, the variability during glacial times is strongly reduced compared to site GeoB 4216.

Maxima in TOC concentration in core GeoB 4216 are accompanied by synchronous changes in other geochemical proxies related to productivity: carbonate concentrations vary between 25% and 80%, and generally are low during TOC maxima. C/N ratios vary between 4 and 8, with glacial OISs 2, end of 3, 6 and 8 yielding generally higher values. Distinct TOC peaks are accompanied by local maxima of C/N. $\delta^{13}C_{org}$ varies between −23.6‰ and −19.9‰. The record shows a long-term decrease between OISs 5 and 1 by about 1‰. Values of $\delta^{15}N$ vary between 4.5‰ and 7.8‰. Values of $\delta^{13}C$ of *C. wuellerstorfi* vary between −0.2‰ and 1.1‰. Local minima of $\delta^{13}C_{org}$, $\delta^{15}N$ and $\delta^{13}C$ of *C. wuellerstorfi* coincide with TOC maxima.

The interpretation of none of these proxies is unequivocal. However, the strong time coincidence of variations suggests a common cause for this variability, as will be discussed later.

4.3. Geochemical results at the near-coastal sites GeoB 4223 and GeoB 4240 (upwelling influenced)

TOC concentrations at sites GeoB 4223 and GeoB 4240 (0.25–1.2%) are higher compared to the offshore stations (Figs. 6 and 7). The general pattern observed in the offshore stations with higher TOC concentrations during glacial times

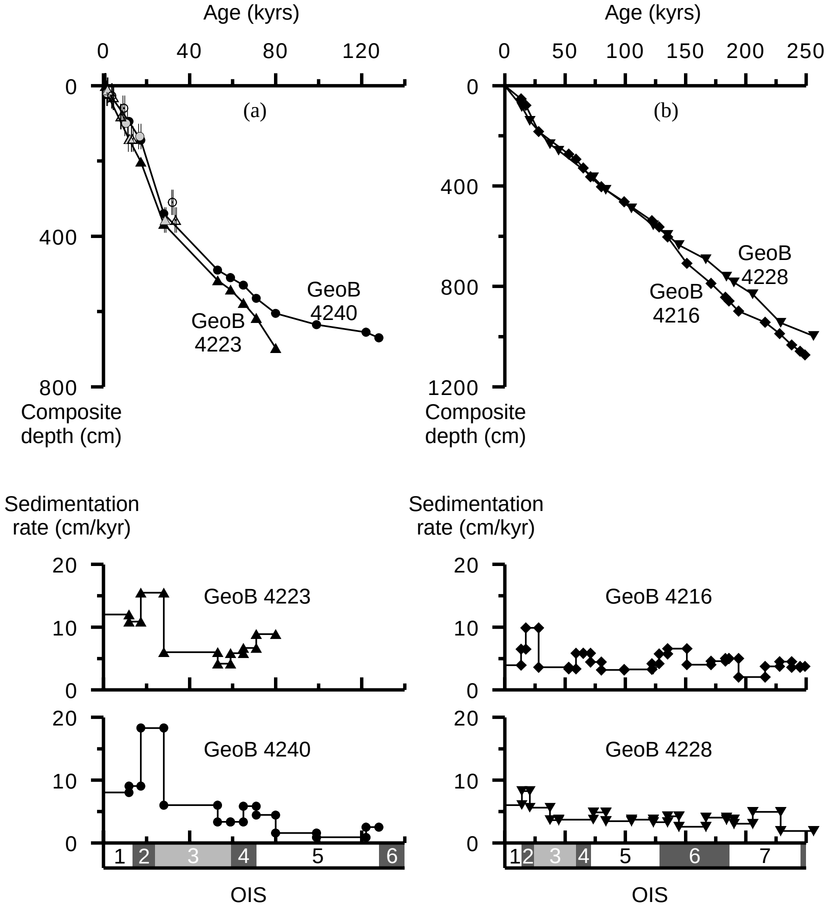

Fig. 4. Age-depth plots and sedimentation-rate estimates for (a) the near-coastal stations GeoB 4223 and GeoB 4240 and (b) the offshore stations GeoB 4216 and GeoB 4228. Black symbols indicate tie points derived from oxygen isotope stratigraphy (cores GeoB 4216, GeoB 4223, GeoB 4240) or from correlation of susceptibility (core GeoB 4228). Grey symbols indicate ^{14}C ages on monospecific *G. bulloides* samples. Open symbols indicate ^{14}C AMS ages of mixed planktic foraminifera samples. ^{14}C AMS ages were calibrated to calendar years BP and are given as 2σ-ranges (95% confidence limit) (see Henderiks et al., 2002).

also is observed in the near-coastal stations. Despite of this similarity remarkable differences were identified: The early Holocene (OIS 1) is characterized at site GeoB 4223 by high TOC concentrations up to 0.8%, and OIS 4 exhibits low TOC concentrations at both sites. TOC peaks P1, P3, and P6 identified in core GeoB 4216 (as marked in Figs. 6 and 7 by broken lines to facilitate comparison) coincide with TOC maxima in cores GeoB 4223 and GeoB 4240. However, a coincidence of TOC peaks could not be detected for site GeoB 4216 peaks P2, P4, and P5.

At the near-coastal stations, both carbonate concentrations and C/N ratios are high during glacial OISs 2, late 3, and 6. These are time intervals with high TOC concentrations. The $\delta^{13}C_{org}$ values are low (about −21‰) during OISs 2, 4, and 6. During interglacial times they range between −20.5‰ and −19.5‰. The $\delta^{15}N$ values are lowest (about 6‰) during OISs 2, late 3, and 6. During interglacial times they are slightly higher, with a maximum in the middle Holocene (up to 7.5‰). The benthic $\delta^{13}C$ of GeoB 4240 (*C. wuellerstorfi*) ranges between 0.5‰ and 1.4‰,

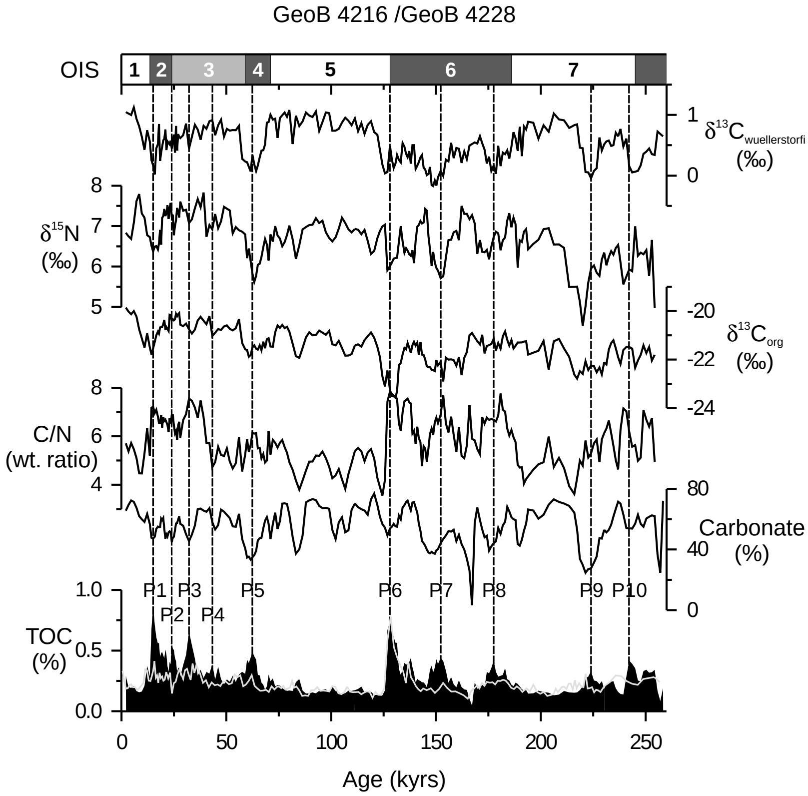

Fig. 5. Geochemical properties in core GeoB 4216 and TOC concentration in core GeoB 4228. TOC concentrations in cores GeoB 4216 and GeoB 4228 are indicated by black shading and grey line, respectively. Broken lines indicate distinct TOC peaks in core GeoB 4216.

with lowest values during OISs 1/2 and 6. The benthic δ^{13}C of GeoB 4223 (*U. peregrina*) ranges between −0.9‰ and 0.9‰. Times of higher TOC concentrations (OIS 3 to early OIS 1) are coincident, with generally lower benthic δ^{13}C values at site GeoB 4223.

5. Discussion

Productivity variations in the upwelling area off NW Africa between 13°N and 32°N during glacial–interglacial cycles have been investigated by various methods using micropaleontological and geochemical proxies (Müller et al., 1983; Sarnthein et al., 1987; Marret and Turon, 1994; Martinez et al., 1996; Guichard et al., 1999; Abrantes, 2000). With the exception of sites located at 20°N (Harris et al., 1996; Guichard et al., 1997; Martinez et al., 1999) increased upwelling was observed during glacial OISs 2, 3, 4, and 6 relative to interglacial OISs 1 and 5. These findings are corroborated by generally higher TOC concentrations and higher sedimentation rates during glacial times at all four investigated sites.

Despite this overall similarity, remarkable differences were observed between the different sites. The highest variability in TOC concentrations was observed at site GeoB 4216. In contrast to core GeoB 4216 the near-shore stations GeoB 4223 and GeoB 4240 show comparably low TOC concentrations during OIS 4. While TOC peaks coincide with minima of carbonate, $\delta^{13}C_{org}$, δ^{15}N, and $\delta^{13}C_{benthic}$ at site GeoB 4216, this observation is

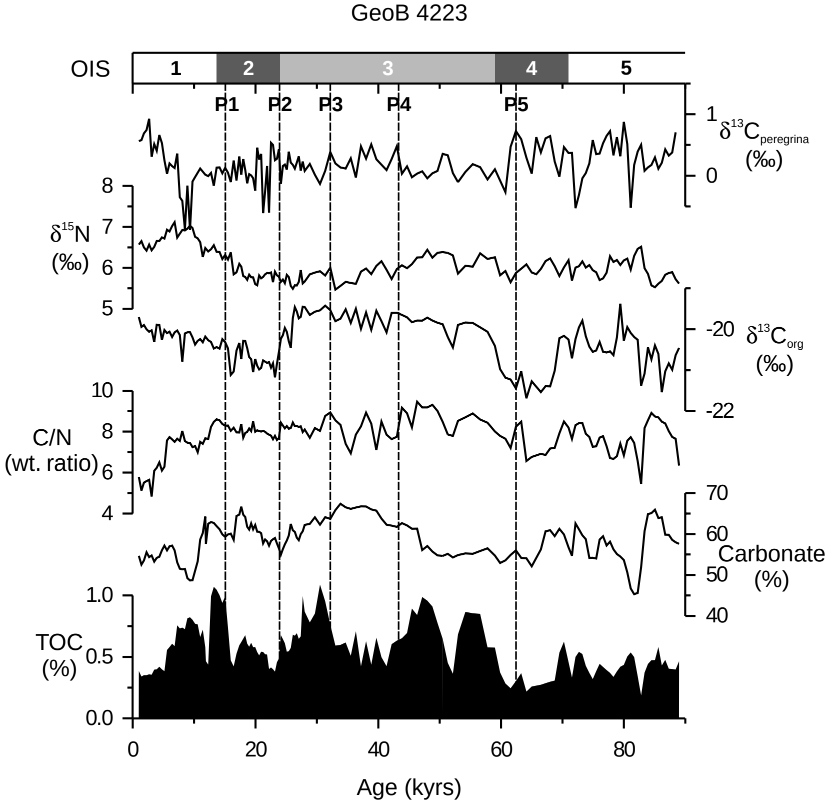

Fig. 6. Geochemical properties in core GeoB 4223. For comparison, times of TOC peaks in core GeoB 4216 are indicated by broken lines.

not generally true for sites GeoB 4223 and GeoB 4240. These differences point to a rather complex sedimentation pattern in the investigation area.

The differences between the productivity records of sites GeoB 4216 and GeoB 4228, with higher TOC concentrations at site GeoB 4216, especially during glacial times, may be explained by the influence of the Cape Ghir filament at this site during times of intensified filament activity. This interpretation is supported by investigations of surface sediments in the investigation area: although lateral particle transport and early diagenesis result in a smoothing of the geochemical productivity signal in the sediments (Freudenthal et al., 2001a), even meso-scale features like the Cape Ghir are reflected in the sediments by proxies related to productivity and nutrient conditions, like TOC concentration and δ^{15}N (Meggers et al., 2002).

If the variations in the productivity record are climatically induced, at least the productivity records of upwelling influenced sites GeoB 4223 and GeoB 4240 should co-vary with the record of site GeoB 4216, since both upwelling intensity and filament activity are dependent on the strength and duration of the trade winds. In the following we discuss, why this co-variation is not seen in the sediments. First, the possible alteration or masking of the marine productivity records by early diagenesis and terrestrial sediment supply is evaluated. Then we discuss the locally varying impact of sea level and climate-induced changes on the sedimentary record of the various geochemical productivity indicators.

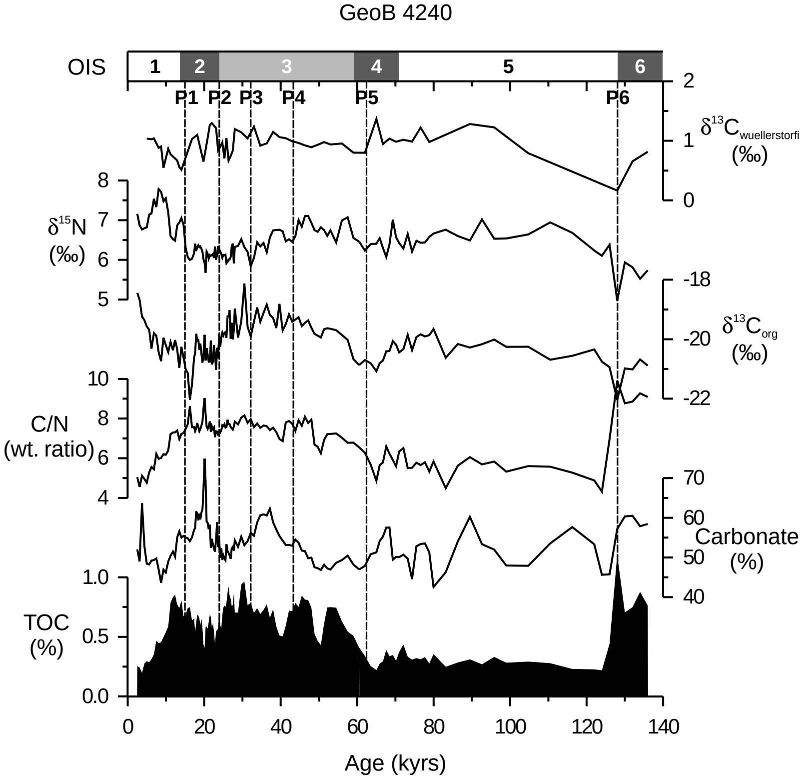

Fig. 7. Geochemical properties in core GeoB 4240. For comparison, times of TOC peaks in core GeoB 4216 are indicated by broken lines.

5.1. Early diagenesis

The remineralization of organic matter in sinking particles and in the sediments has a major impact on sedimentary TOC concentrations, on C/N ratios, and the stable nitrogen and carbon isotope ratios (Tyson, 1995). Organic matter degradation in marine sediments causes an increase of pCO_2 in pore waters, which may result in carbonate dissolution even in sediments located above the carbonate lysocline (Jahnke et al., 1994; Milliman et al., 1999). Thus changes in organic-matter preservation would cause synchronous changes in organic geochemical proxies and carbonate concentrations as observed in GeoB 4216.

Reduced bottom-water oxygenation as indicated by lower $\delta^{13}C$ of epibenthic foraminifera, due to a decrease of NADW formation especially during terminations, could account for enhanced organic-matter preservation (Sarnthein and Tiedemann, 1990; Sarnthein et al., 1994). Oxygen concentrations off Portugal at similar water depths compared to this study may have dropped from recently 5–6 μM/l to <0.5 μM/l during distinct intervals of OISs 2 and 3 (Baas et al., 1998). Site GeoB 4216 (2300 m water depth) is influenced by NADW, while sites GeoB 4223 (770 m), GeoB 4240 (1360 m), and GeoB 4228 (1600 m) are situated in the depth range of the MOW. Changes of organic-matter preservation at site GeoB 4216 due to changes of NADW production, therefore, could explain the differences in the organic geochemical profiles at this site compared to the MOW influenced sites. However, the upwelling-influenced site GIK 12392 (25°N, 2575 m water depth) should have experienced similar bottom-water oxygenation variations as site GeoB 4216, although the variability of TOC concentrations resembles those of GeoB 4228 and GeoB 4240 with high concentrations during OISs 2,3, and 6 and low concentrations during OISs 1,4, and 5 (Müller and Suess, 1979). In addition to bottom-water oxygen concentration, the influence of mineralogy, specific surface area of lithogenic matter, and lithogenic matter sedimentation are discussed as main factors controlling organic-matter preservation (Hedges and Keil, 1995; Ransom et al., 1998; Cowie et al., 1999). Lithogenic sedimentation off NW Africa adjacent to the Sahara is mainly controlled by dust. Therefore, we do not expect small-scale regional variations in the pattern of lithogenic matter sedimentation, which would be necessary to explain the differences in TOC concentrations at sites GeoB 4216 and GeoB 4228 by preservation. We conclude that regional changes in organic matter preservation were not caused by changes in bottom-water oxygenation or by changes in lithogenic sedimentation, but by local changes in organic matter supply. Similarly, Martinez et al. (1996) concluded from an integrated study of organic and inorganic productivity proxies at an upwelling-influenced site south of our investigation area at 25°N that these proxies reflect primarily changes in their supply despite of the severe impact of early diagenesis.

5.2. Terrestrial organic matter supply versus marine productivity

In many studies the sedimentary organic carbon has been proven to be a highly valuable and reliable indicator in highly productive continental margin areas if the impact of terrestrial organic matter has minor importance (Rühlemann et al., 1999). Terrestrial particles are mainly transported to the northern Canary basin as dust, while river transport is of minor importance in this area adjacent to the semi-arid to arid NW African continent. Typical carbonate variations in the North Atlantic with low concentrations during glacial times and cold periods of interglacial times, as are observed at the offshore site GeoB 4216, have been related to dilution by increased dust supply (Bacon, 1984; Francois et al., 1990; Matthewson et al., 1995). Dissolution has a minor impact on carbonate variability at site GeoB 4216 (Henderiks et al., 2002). At the near-coastal sites GeoB 4223 and GeoB 4240 high carbonate concentrations during OISs 2 and 4 may be explained either by upwelling-influenced biogenic carbonate production that exceeds increased dust supply during glacial times, or by increased detritical carbonate sedimentation (Henderiks et al., 2002).

Dust consists mainly of lithogenic components, but also of smaller amounts of biogenic components containing terrestrial organic matter. Thus, the question arises, can the observed variability of TOC concentrations at site GeoB 4216, which is coincident with increased dust supply indicated by low carbonate concentrations, be explained by terrestrial organic matter sedimentation?

Sedimentary C/N ratios and $\delta^{13}C_{org}$ values are widely used to distinguish between marine and terrestrial organic matter. Typical terrigenous C/N ratios are >20, whereas marine ratios range from 5 to 10 (Tyson, 1995). However, the analysis of sedimentary C/N ratios allows only rough estimates of the relative contribution of terrestrial organic matter, due to preferential degradation of nitrogen-enriched organic compounds and the influence of inorganic nitrogen on sedimentary C/N ratios. $\delta^{13}C_{org}$ may be used for quantification if the influence of C4-plant material can be neglected and if the different isotope ratios of the marine and terrestrial end members are known (Wagner and Dupont, 1999). Pollen investigations indicate that terrestrial organic matter sedimentation in the northern Canary Basin is dominated by C3-plants from the Mediterranean realm (Hooghiemstra et al., 1992). C3-plants reveal low $\delta^{13}C_{org}$ values between −25.5‰ and −29.3‰, with an average of −27‰ (Tyson, 1995). A single measurement on dust sampled in the vicinity of the Canary Islands resulted in a terrestrial $\delta^{13}C_{org}$ of −25‰ (T.F., unpublished data). The stable carbon isotope ratio of marine organic matter of low and middle latitudes range typically from −18.5‰ to −21.5‰ (Sackett, 1986). Part of the variability of the marine $\delta^{13}C_{org}$ signature may be explained by varying pCO_2 due to glacial/interglacial changes in the atmospheric CO_2 content or in upwelling intensity (Rau et al., 1989; Müller et al., 1994).

In our study C/N ratios between 4 and 10 and $\delta^{13}C_{org}$ values between −23.5‰ and −19‰ indicate a general dominance of marine organic matter in the sediments. This interpretation is supported by microscopic investigations of the organic matter in sediments off NW Africa (Martinez et al., 1999; Freudenthal et al., 2001b). The variability observed in $\delta^{13}C_{org}$ may be attributed both to variations in the terrestrial organic matter supply and to changes in the productivity conditions related to upwelling activity and filament intensity, both of which are dependent on the intensity of the trade winds.

The high sensitivity of $\delta^{15}N$ to nutrient supply has been shown in various upwelling regions of the world ocean (Altabet and Francois, 1994; Holmes et al., 1998; Hebbeln et al., 2000). According to preferential assimilation of $^{14}NO_3^-$ and Rayleigh fractionation kinetics, an increased supply of nitrate causes lower $\delta^{15}N$ values in the marine organic matter (Altabet and Francois, 1994). Other possible factors influencing the sedimentary $\delta^{15}N$ seem to be of minor importance: Changes in $\delta^{15}N$ of nitrate due to changes in the global nutrient cycling should affect all investigated sites in the same manner (Altabet and Curry, 1989; Kienast, 2000); a significant impact of ^{15}N-depleted inorganic nitrogen in organic-poor sediments of the investigation area would be contrary to our observations in low sedimentary $\delta^{15}N$ with low TOC concentrations and low C/N ratios (Freudenthal et al., 2001b).

In some cases, ^{15}N-depleted sedimentary stable nitrogen isotope ratios also have been used as an indicator of terrestrial organic matter (Sweeney and Kaplan, 1980; Mariotti et al., 1984). Thus, similar to $\delta^{13}C_{org}$, the variability of sedimentary $\delta^{15}N$ can be attributed both to variations in the terrestrial organic matter supply and to changes in productivity conditions. However, $\delta^{15}N$ is less sensitive to variations in terrestrial organic matter, since marine organic matter yields much higher nitrogen concentrations. Regarding the general dominance of marine organic matter in the sediments of our investigation area, we interpret variations of $\delta^{15}N$ as indicator of nutrient supply related to variations in upwelling intensity and filament transport. Increased nutrient supply was responsible for increased productivity as shown by low $\delta^{15}N$ and high TOC concentrations at OISs 2 and 3 in the upwelling-influenced sites GeoB 4223 and GeoB 4240, and a general coincidence of $\delta^{15}N$ minima and TOC maxima at the offshore site GeoB 4216 during glacial periods.

We conclude that variations in TOC concentrations reflect the variability in marine productivity. The much higher variability observed at the offshore site GeoB 4216 compared to site GeoB 4228 indicates that local productivity processes (not dust supply, which should have similar signals in both offshore sites) related to the Cap Ghir filament activity are documented in TOC concentrations of core GeoB 4216.

Additional evidence for the interpretation of TOC concentrations at core GeoB 4216 as a marine productivity signal reflecting filament activity is provided by the analysis of the gradient in $\delta^{18}O$ of planktic foraminifera between site GeoB 4216 and the upwelling-influenced sites GeoB 4223 and GeoB 4240 (Fig. 8). This gradient is independent of organic matter degradation or terrestrial sediment supply. The $\delta^{18}O$ is dependent on the global variability of the hydrological cycle documented in sea-level variations, and is further dependent on the local surface-water density (e.g., Billups and Schrag, 2000), which is a function of salinity and temperature. A strong density gradient exists between coastal-upwelled and offshore subtropical gyre surface waters partly due to changes in salinity induced by evaporation (Hagen et al., 1996). The density gradient between the filament-influenced site GeoB 4216 and the upwelling-influenced sites GeoB 4223 and GeoB 4240 should be small if upwelled water was transported within the Cape Ghir filament region offshore to site GeoB 4216, and should be stronger if filament activity was weak and did not influence this site. Examination of the $\delta^{18}O$ gradient reveals lowest gradients between the end of OISs 3 and 2, where highest TOC concentrations at GeoB 4216 and thus strongest filament activity was observed (Fig. 8), supporting the interpretation of TOC variability at site GeoB 4216 as filament signal.

5.3. Influence of sea-level changes and trade winds on the productivity signal

Productivity variations related to coastal upwelling and to the Cape Ghir filament depend on the

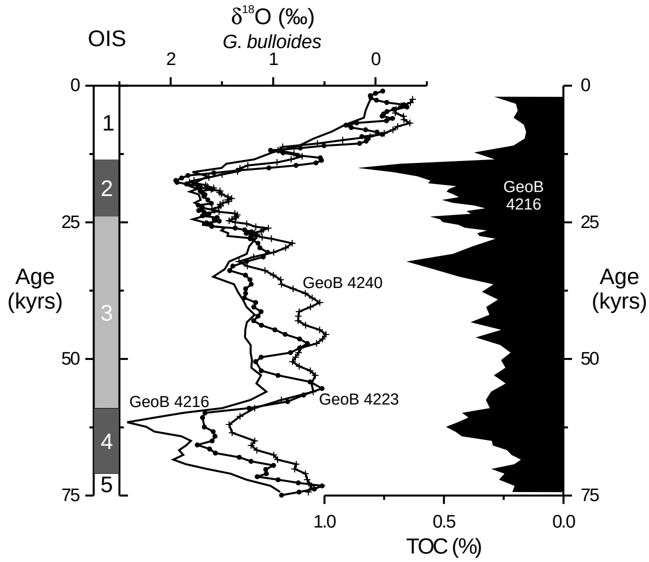

Fig. 8. Comparison of smoothed $\delta^{18}O$ of *G. bulloides* (5-point least-square smoothing using the program AnalySeries; Paillard et al., 1996) at the upwelling-influenced sites GeoB 4223 and GeoB 4240 and at the filament-influenced site GeoB 4216 as related to TOC variations at site GeoB 4216.

strength of the NE trade wind system in the investigation area. If the regional climate were the only factor influencing the sedimentary productivity record, variations in productivity proxies should co-vary at the coastal upwelling-influenced sites GeoB 4223 and GeoB 4240, and at the filament-influenced site GeoB 4216. As already pointed out, this is not the case. Another factor with different regional impact on the different investigation sites is needed to explain the observed dissimilarity. Sea-level change could be an important additional factor. Four major processes have to be considered:

1. Sea-level changes are responsible for zonal shifts of the centers of upwelling and filament activity. During glacial times lowered sea level caused a shift in the shoreline and the upwelling center towards the shelf edge, that is towards the study area (compare Guichard et al., 1999).
2. Sea-level changes should have an impact on the nutrient content of upwelled waters. During interglacial times, when upwelling is centered on the shelf, upwelled waters would have been in contact with the shelf, where much of the nutrient regeneration occurs. This contact was less important during glacial times, when much of shelf area was subaerially exposed (Bertrand et al., 2000).
3. Most of the particle production on the shelf is deposited in the upper part of the continental slope during interglacial sea-level high stands. During glacial times, when the shelf was much narrower, different modes of lateral particle transport and deposition on the continental shelf and slope area may have been active (Fütterer, 1983). Erosion of shelf sediments during glacial low sea level could explain increased detritical particle sedimentation on the slope (Henderiks et al., 2002).
4. Changes in sea level and consequent changes in coastal and shelf topography likely influence filament activity. Preliminary results obtained with an eddy-permitting high-resolution regional oceanographic model of the Canary Islands region show that filament formation in the Cape Ghir region does not subside even during glacials when sea level is 100 m below present (I. Stevens, pers. comm.).

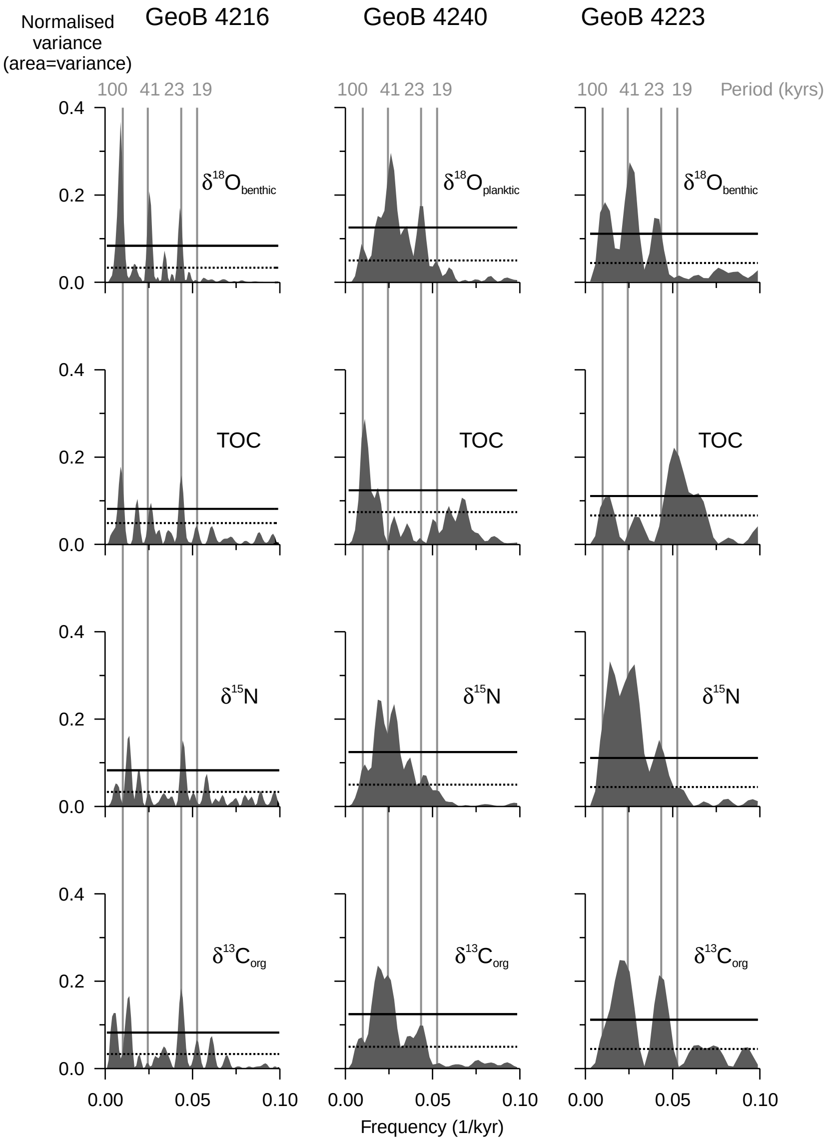

Fig. 9. Power spectra of $\delta^{18}O$, TOC concentrations, $\delta^{15}N$, and $\delta^{13}C_{org}$ in cores GeoB 4216, GeoB 4223, and GeoB 4240. Spectra were calculated from harmonic analyses of each parameter after Schulz and Stattegger (1997) without time-interpolation (6 dB bandwidth [site GeoB 4216: 0.005 ka^{-1}; site GeoB 4240: 0.009 ka^{-1}; site GeoB 4223: 0.014 ka^{-1}]; significance level $\alpha = 0.01$; linear trend subtracted) Horizontal lines indicate critical levels for the Fisher test (Fisher, 1929). Grey bars mark Milankovitch frequencies.

Power spectra may help distinguish the climate-induced variability of the productivity records from the sea-level-induced variability. Sea-level changes are mainly reflected by the benthic and planktic $\delta^{18}O$ records. The power spectra of the $\delta^{18}O$ records are dominated by variances at orbital periodicity related to eccentricity and obliquity ($T = 100$ and 41 ka, respectively) and to minor amounts related to precession ($T = 23$ ka). The dominance of the obliquity signal is seen at all three sites GeoB 4216, GeoB 4223, and GeoB 4240 (Fig. 9). The eccentricity is only detected at site GeoB 4216 depending on the length of the time series.

TOC, $\delta^{15}N$ and $\delta^{13}C_{org}$ profiles at site GeoB 4216 are characterized by a higher relative variance at the precessional frequency, which shows significant coherence (0.1 significance level) and negligible phase shift ($3.5 \pm 23.2°$ for $\delta^{15}N$, $12.6 \pm 18.6°$ for $\delta^{13}C_{org}$, both versus TOC) according to cross-spectral analysis (using the software Spectrum by Schulz and Stattegger, 1997). While the obliquity signal is still significant with regard to TOC, it is not detected at the $\delta^{15}N$ and $\delta^{13}C_{org}$ profiles. Sea-level change seems to have a minor impact on the accumulation of organic matter and its geochemical signature at this site. Instead, frequency analyses indicate a strong precessional forcing on productivity.

At the upwelling influenced sites GeoB 4223 and GeoB 4240 a strong obliquity component is observed both in the $\delta^{15}N$ and $\delta^{13}C_{org}$ profiles, which indicates an impact of sea-level changes on these proxies at the near-coastal sites. Low $\delta^{15}N$ and $\delta^{13}C_{org}$ values were observed during OISs 2, 3 (low $\delta^{15}N$ but high $\delta^{13}C_{org}$), 4, and 6, that is during times of low sea level. With respect to $\delta^{15}N$, the impact of sea level is best explained by a lateral shift of the upwelling center towards the investigation sites during lowered sea level. A decrease of sedimentary $\delta^{15}N$ towards the upwelling center, due to increased concentrations of upwelled nitrate and preferential assimilation of $^{14}NO_3^-$, is a general feature observed in upwelling systems (e.g., Altabet and Francois, 1994; Hebbeln et al., 2000; Holmes et al., 1998; Meggers et al., 2002). The coincident decrease of $\delta^{13}C_{org}$ may be explained in analogy by increased concentrations of CO_2 due to the shift of the upwelling center towards the study area. In addition to the obliquity signal indicating the impact of sea-level changes, precessional forcing is still recognized at the TOC, $\delta^{15}N$ and $\delta^{13}C_{org}$ profiles of core GeoB 4223. No indication of precessional forcing on productivity was found at site GeoB 4240. The strong sensitivity of sites GeoB 4223 and GeoB 4240 to longitudinal shifts of the coastal upwelling in combination with the impact of changing nutrient concentrations of the upwelled waters and changing shelf and slope deposition patterns, all related to sea-level changes, can explain the differences in the productivity records of cores GeoB 4216, GeoB 4223, and GeoB 4240.

At the filament-influenced site GeoB 4216 strong time-coherence of different proxies related to productivity indicates the dominance of a single process on the productivity record. At the upwelling-influenced continental slope sites GeoB 4223 and GeoB 4240 the lack of coherence between different productivity proxies indicates that at least two factors influence the productivity record, with different proxies reacting with different sensitivity on changes of these factors. We assume that upwelling intensity and filament activity are controlled by the same precessional forcing mechanism. However, this forcing mechanism is masked at the near-coastal sites by the strong impact of sea-level change on the productivity signal. In contrast, site GeoB 4216 seems to be a highly sensitive recorder of productivity variations related to Cape Ghir filament intensity and thus related to NE trade-wind strength.

Analysis of the Si/Al ratio at site GeoB 4216 and pollen at a nearby station (site GIK 16004, see

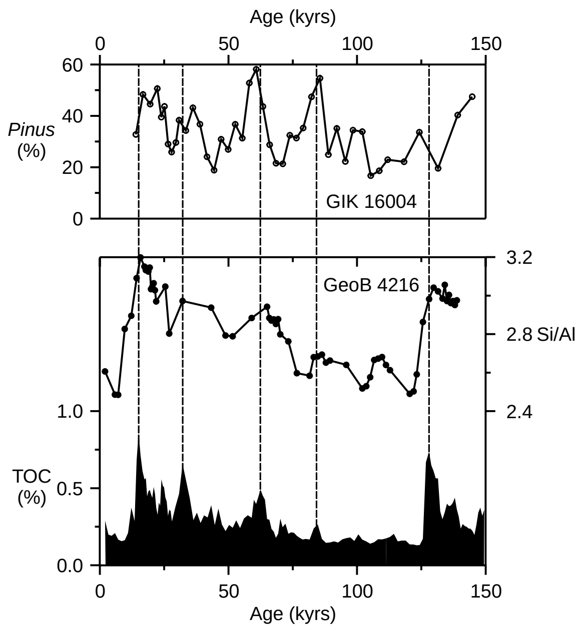

Fig. 10. Comparison of TOC variability at the filament-influenced site GeoB 4216 with the Si/Al ratio in the same core and trade winds indicated by percentages of *Pinus* pollen (Hooghiemstra et al., 1992) in a nearby sediment core.

Fig. 1 for location) supports the interpretation of a relationship between trade-wind and productivity variations at site GeoB 4216 (Fig. 10). The Si/Al ratios in these biogenially Si-poor sediments are related to the grain-size of the lithogenic fraction (Martinez et al., 1999), higher Si/Al ratios being correlated with coarser grain sizes and higher TOC concentrations (Moreno et al., submitted). Cross spectral analysis of the Si/Al ratio and TOC concentration at site GeoB 4216 reveal strong coherence in the precessional and eccentricity frequency range, which is explained by strongest trade winds during times of maximum summer insolation in the Northern Hemisphere and during Terminations I and II (Moreno et al., submitted). Peaks in the abundance of *Pinus* pollen at site GIK 16004, which originate from the Mediterranean vegetation belt and can be used as a trade-wind indicator (Hooghiemstra et al., 1992; Dupont, 1999), coincide with TOC peaks in core GeoB 4216. Thus, productivity and grain size proxies at site GeoB 4216, together with pollen at site GIK16004, are indicative for a precessional forcing of summer trade winds off NW Africa.

6. Conclusions

Despite early diagenesis and lateral particle transport, sedimentary geochemical properties reflect mainly productivity gradients in the investigation area adjacent to the upwelling area off Morocco, allowing at least a qualitative reconstruction of late Quaternary productivity variations. The productivity records at the four sites investigated in this study showed both similarities and differences. The observed general pattern, of higher marine productivity during glacial times, is similar at all four sites. However, detailed examination of the records reveals strong differences in the variability of productivity during glacial times, indicating different forcing mechanisms.

Two different processes were identified that influence the productivity record: global sea-level changes control the distance of the investigation site to the upwelling zone, while the strength of summer NE Trades is determinant for the upwelling intensity. The impact of sea-level changes strongly overprints the regional climatic signal on the continental slope. In contrast, the productivity record of an offshore site influenced by the upwelling-related Cape Ghir filament is highly sensitive to changes in trade-wind intensity. Summer trade-wind intensity off NW Africa seems to be related to precessional forcing mechanisms.

A careful selection of the investigation site is needed for the investigation of paleointensity of coastal upwelling. A dominance of sea-level change on the productivity record largely overprinting the paleoclimatic signal has to be considered for all continental margins that are characterized by a broad shelf.

Acknowledgements

The authors thank the crew aboard R.V. *METEOR* for the help during coring of sediments. We are grateful to D. Hebbeln for intensive discussions and helpful suggestions on an earlier version of this manuscript. We thank W. Berger and an anonymous reviewer for helpful comments. We acknowledge the assistance in the laboratory work of M. Segl, H. Buschoff, J. Thiele, A. Eberwein and P. Franke. Data presented in this study are available at the CANIGO data center and under www.pangaea.de/home/tfreudenthal/. This research was funded by the European Commission (MAST III Programme CANIGO, MAS3-CT96-0060) and the "Deutsche Forschungsgemeinschaft" (DFG Grant no. We 992/31-1).

References

Abrantes, F., 2000. 200,000 yr diatom records from Atlantic upwelling sites reveal maximum productivity during LGM and a shift in phytoplankton community structure at 185,000 yr. Earth and Planetary Science Letters 176 (1), 7–16.

Altabet, M.A., Curry, W.B., 1989. Testing models of past ocean chemistry using foraminifera $^{15}N/^{14}N$. Global Biogeochemical Cycles 3 (2), 107–119.

Altabet, M.A., Francois, R., 1994. Sedimentary nitrogen isotopic ratio as a recorder for surface ocean nitrate utilization. Global Biogeochemical Cycles 8 (1), 103–116.

Baas, J.H., Schönfeld, J., Zahn, R., 1998. Mid-depth oxygen drawdown during Heinrich events: evidence from benthic foraminiferal community structure, trace-fossil tiering, and benthic $\delta^{13}C$ at the Portuguese Margin. Marine Geology 152 (1–3), 25–55.

Bacon, M.P., 1984. Glacial to interglacial changes in carbonate and clay sedimentation in the Atlantic Ocean estimated from ^{230}Th measurements. Isotope Geoscience 2, 97–111.

Bard, E., Fairbanks, R., Arnold, M., Maurice, P., Duprat, J., Moyes, J., Duplessy, J.-C., 1989. Sea-level estimates during the last deglaciation based on $\delta^{18}O$ and accelerator mass spectrometry ^{14}C ages measured in *Globigerina bulloides*. Quaternary Research 31, 381–391.

Bertrand, P., Pedersen, T.F., Martinez, P., Calvert, S., Shimmield, G., 2000. Sea level impact on nutrient cycling in coastal upwelling areas during deglaciation: evidence from nitrogen isotopes. Global Biogeochemical Cycles 14 (1), 341.

Billups, K., Schrag, D.P., 2000. Surface ocean density gradients during the Last Glacial Maximum. Paleoceanography 15 (1), 110.

Cowie, G.L., Calvert, S.E., Pedersen, T.F., Schulz, H., von Rad, H., 1999. Organic content and preservational controls in surficial shelf and slope sediments from the Arabian Sea (Pakistan margin). Marine Geology 161, 23–38.

Davenport, R., Neuer, S., Hérnandez-Guerra, A., Rueda, M.J., Llinas, O., Fischer, G., Wefer, G., 1999. Seasonal and interannual pigment concentration in the Canary Islands region from CZCS data and comparison with observations from the ESTOC. International Journal of Remote Sensing 20 (7), 1419–1433.

Dupont, L.M., 1999. Pollen and spores in marine sediments from the East Atlantic. A view from the ocean into the African continent. In: Fischer, G., Wefer, G. (Eds.), Use of Proxies in Paleoceanography: Examples from the South Atlantic. Springer, Berlin, Heidelberg, pp. 523–546.

Fairbanks, R.G., 1989. A 17,000 year glacio-eustatic sea level record: influence of glacial melting rates on the Younger Dryas event and deep-ocean circulation. Nature 342, 637–642.

Fischer, G., cruise participants, 1997. Report and preliminary results of Meteor-cruise M 38/1, Las Palmas-Recife, 25.1.-1.3.1997. Berichte, 94. Fachbereich Geowissenschaften, Universität Bremen, Bremen, 178 pp.

Fisher, R.A., 1929. Tests of significance in harmonic analysis. Proceedings of the Royal Society of London, Series A 125, 54–59.

Francois, R., Bacon, M.P., Suman, D.O., 1990. Thorium 230 profiling in deep-sea sediments: high-resolution records of flux and dissolution of carbonate in the equatorial Atlantic during the last 24,000 years. Paleoceanography 5, 761–787.

Freudenthal, T., Neuer, S., Meggers, H., Davenport, R., Wefer, G., 2001a. Influence of lateral particle advection and organic matter degradation on sediment accumulation and stable nitrogen isotope ratios along a productivity gradient in the Canary Islands region. Marine Geology 177 (1–2), 93–109.

Freudenthal, T., Wagner, T., Wenzhöfer, F., Zabel, M., Wefer, G., 2001b. Diagenetic fractionation of stable nitrogen and carbon isotopes in surface sediments of the eastern subtropical Atlantic. Geochimica et Cosmochimica Acta 65, 1795–1808.

Fütterer, D.K., 1983. The modern upwelling record off northwest Africa. In: Thiede, J., Suess, E. (Eds.), Coastal Upwelling. Its Sediment Record. Part B: Sedimentary Records of Ancient Coastal Upwelling. NATO Conference Series, Series IV: Marine Science 10b. Plenum Press, New York, London, pp. 105–121.

Guichard, S., Jorissen, F., Bertrand, P., Gervais, A., Martinez, P., Peypouquet, J., Pujol, C., Vergnaud-Grazzini, C., 1997. Foraminiferes benthiques et paleoproductivite: reflexions sur une carotte de l'upwelling (NW africain). Comptes Rendus de l'Académie des Sciences, Series IIA, Earth and Planetary Science 325 (1), 65–70.

Guichard, S., Jorissen, F., Peypouquet, J.-P., 1999. Late Quaternary benthic foraminiferal records testifying lateral variability of the Cape Blanc upwelling signal. Comptes Rendus de l'Académie des Sciences, Series IIA, Earth and Planetary Science 329 (4), 295–301.

Hagen, E., Zülicke, C., Feistel, R., 1996. Near-surface structures in the Cape Ghir filament off Morocco. Oceanologica Acta 19 (6), 577–598.

Harris, P.G., Zhao, M., Rosell-Melé, A., Tiedemann, R., Sarnthein, M., Maxwell, J.R., 1996. Chlorin accumulation rate as a proxy for Quaternary marine primary productivity. Nature 383, 63–65.

Hebbeln, D., Marchant, M., Freudenthal, T., Wefer, G., 2000. Surface sediment distribution along the Chilean continental slope related to upwelling and productivity. Marine Geology 164 (3–4), 119–137.

Hedges, J.I., Keil, R.G., 1995. Sedimentary organic matter preservation: an assesment and speculative synthesis. Marine Chemistry 49, 81–115.

Henderiks, J., Freudenthal, T., Meggers, H., Abrantes, F., Nave, Silvia, Salqueiro, E., Freitas, P., Bollmann, J., Thierstein, H.R., 2002. Glacial–interglacial variability of particle accumulation in the Canary Basin: a time-slice approach. Deep-Sea Research II 49 (17), 3675–3705.

Holmes, M.E., Müller, P.J., Schneider, R.R., Segl, M., Wefer, G., 1998. Spatial variations in euphotic zone nitrate utilization based on $\delta^{15}N$ in surface sediments. Geo-Marine Letters 18, 58–65.

Hooghiemstra, H., Stalling, H., Agwu, C.O.C., Dupont, L.M., 1992. Vegetational and climatic changes at the northern fringe of the Sahara 250,000–5000 years BP: evidence from 4 marine pollen records located between Portugal and the Canary Islands. Review of Paleobotany and Palynology 74, 1–53.

Hughen, K.A., Overpeck, J.T., Peterson, L.C., Trumbore, S., 1996. Rapid climatic changes in the tropical Atlantic region during the last deglaciation. Nature 380, 51–54.

Imbrie, J., Hays, J.D., Martinson, D.G., McIntyre, A., Mix, A.C., Morley, J.J., Pisias, N.G., Prell, W.L., Shackleton, N.J., 1984. The orbital theory of Pleistocene climate: support from a revised chronology of the marine d18O record. In: Berger, A.L., Imbrie, J., Hays, J., Kukla, G., Saltzman, B. (Eds.), Milankovitch and Climate: Understanding the Response to Astronomical Forcing. D. Reidel Publishing Company, Dordrecht, pp. 269–305.

Jahnke, R.A., Craven, D.B., Gaillard, J.-F., 1994. The influence of organic matter diagenesis on $CaCO_3$ dissolution at the deep-sea floor. Geochimica et Cosmochimica Acta 58 (13), 2799–2809.

Johnson, J., Stevens, I., 2000. A fine resolution model of the eastern North Atlantic between the Azores, the Canary Islands and the Gibraltar Strait. Deep Sea Research I 47 (5), 875–899.

Kienast, M., 2000. Unchanged nitrogen isotopic composition of organic matter in the South China Sea during the last climatic cycle: global implications. Paleoceanography 15 (2), 244–253.

Knoll, M., Lenz, B., Lopez Laatzen, F., Müller, T.J., Siedler, G., 2002. The Eastern Boundary Current System between the Canary Islands and the African coast. Deep-Sea Research II 49 (17), 3427–3440.

Lutjeharms, J.R.E., Meeuwis, J.M., 1987. The extent and variability of south-east Atlantic upwelling. In: Payne, A.I.L., Gulland, J.A., Brink, K.H. (Eds.), The Benguela and Comparable Ecosystems. South African Journal of Marine Science, Vol. 5, pp. 51–62.

Mariotti, A., Lancelot, C., Billen, G., 1984. Natural isotopic composition of nitrogen as a tracer of origin for suspended organic matter in the Scheldt estuary. Geochimica et Cosmochimica Acta 48, 549–555.

Marret, F., Turon, J.-L., 1994. Paleohydrology and paleoclimatology off Northwest Africa during the last glacial–interglacial transition and the Holocene: palynological evidences. Marine Geology 118, 107–117.

Martinez, P., Bertrand, P., Bouloubassi, I., Bareille, G., Shimmield, G., Vautravers, B., Grousset, F., Guichard, S., Ternoys, Y., Sicre, M.-A., 1996. An integrated view of inorganic and organic biogeochemical indicators of paleoproductivity changes in a coastal upwelling area. Organic Geochemistry 24, 411–420.

Martinez, P., Bertrand, P., Shimmield, G.B., Cochrane, K., Jorissen, F.J., Foster, J., Dignan, M., 1999. Upwelling intensity and ocean productivity changes off Cape Blanc (northwest Africa) during the last 70,000 years: geochemical and micropalaeontological evidence. Marine Geology 158 (1–4), 57–74.

Matthewson, A.P., Shimmield, G.B., Kroon, D., Fallick, A.E., 1995. A 300 kyr high-resolution aridity record of the North African continent. Paleoceanography 10 (3), 677–692.

McCreary, J.P., Fukamachi, Y., Kundu, P.K., 1991. A numerical investigation of jets and eddies near an eastern ocean boundary. Journal of Geophysical Research 96 (C2), 2515–2534.

Meggers, H., Freudenthal, T., Nave, S., Targarona, J., Abrantes, F., Helmke, P., 2002. Assessment of geochemical and micropaleontological sedimentary parameters as proxies of surface water properties in the Canary Islands region. Deep-Sea Research II 49 (17), 3631–3654.

Milliman, J.D., Troy, P.J., Balch, W.M., Adams, A.K., Li, Y.-H., Mackenzie, F.T., 1999. Biologically mediated dissolution of calcium carbonate above the chemical lysocline? Deep-Sea Research I 46, 1653–1669.

Mittelstaedt, E., 1991. The ocean boundary along the northwest African coast: circulation and oceanographic properties at the sea surface. Progress in Oceanography 26, 307–355.

Moreno, A., Targarona, J., Henderiks, J., Canals, M., Freudenthal, T., Meggers, H., 2001. Orbital forcing of dust supply to the North Canary Basin over the last 250 kyrs. Quaternary Science Reviews 20, 1327–1339.

Müller, P.J., Suess, E., 1979. Productivity, sedimentation rate, and sedimentary carbon content in the oceans. Deep-Sea Research 26A, 1347–1362.

Müller, P.J., Erlenkeuser, H., von Grafenstein, R., 1983. Glacial–interglacial cycles in oceanic productivity inferred from organic carbon contents in eastern North Atlantic sediments. In: Thiede, J., Suess, E. (Eds.), Coastal Upwelling. Its Sediment Record. Part B: Sedimentary Records of Ancient Coastal Upwelling. NATO Conference Series, Series IV: Marine Science 10b. Plenum Press, New York, London, pp. 365–398.

Müller, P.J., Schneider, R., Ruhland, G., 1994. Late quaternary pCO_2 variations in the Angola Current: evidence from organic carbon $\delta^{13}C$ and alkenone temperatures. In: Zahn, R., Pedersen, T.F., Kaminski, M.A., Labeyrie, L. (Eds.), Carbon Cycling in the Glacial Ocean: Constraints of the Ocean's Role in Global Change. NATO ASI Series. Springer, Berlin, Heidelberg, pp. 343–366.

Müller, T.J., Llinas, O., López Laatzen, F., Hernandez Guerra, A., 1999. The eastern boundary current system from eulerian measurements, CANIGO Conference Las Palmas de Gran Canaria. 12–16 Septembre 1999. Book of Abstracts, p. 82.

Nykjær, L., Van Camp, L., 1994. Seasonal and interannual variability of coastal upwelling along northwest Africa and Portugal from 1981 to 1991. Journal of Geophysical Research 99 (C7), 14197–14207.

Paillard, D., Labeyrie, L., Yiou, P., 1996. Macintosh program performs time-series analysis. Eos Transactions AGU 77, 379.

Ransom, B., Kim, D., Kastner, M., Wainwright, S., 1998. Organic matter preservation on continental slopes: importance of mineralogy and surface area. Geochimica et Cosmochimica Acta 62 (8), 1329.

Rau, G.H., Takahashi, T., Des Marais, D.J., 1989. Latitudinal variations in plankton $\delta^{13}C$: implications for CO_2 and productivity in past oceans. Nature 341, 516–518.

Raymo, M.E., 1997. The timing of major climate terminations. Paleoceanography 12 (4), 577–585.

Rühlemann, C., Müller, P.J., Schneider, R.R., 1999. Organic carbon and carbonate as paleoproductivity proxies: examples from high and low productivity areas of the tropical Atlantic. In: Fischer, G., Wefer, G. (Eds.), Use of Proxies in Paleoceanography: Examples from the South Atlantic. Springer, Berlin, Heidelberg, pp. 315–344.

Sackett, W.M., 1986. Stable carbon isotope studies on OM in the marine environment. In: Fontes, P.F., Fritz, J.C. (Eds.), Handbook of Environmental Isotope Geochemistry. Elsevier, Amsterdam, pp. 139–169.

Sarnthein, M., Tiedemann, R., 1990. Younger Dryas-style cooling events at glacial terminations I–IV at ODP site 658: associated benthic $\delta^{13}C$ anomalies constrain meltwater hypothesis. Paleoceanography 5 (6), 1041–1055.

Sarnthein, M., Thiede, J., Pflaumann, U., Erlenkeuser, H., Fütterer, D., Koopmann, B., Lange, H., Seibold, E., 1982. Atmospheric and oceanic circulation patterns off Northwest Africa during the past 25 million years. In: von Rad, U., Hinz, K., Sarnthein, M., Seibold, E. (Eds.), Geology of the Northwest African Continental Margin. Springer, Berlin, Heidelberg, pp. 545–604.

Sarnthein, M., Winn, K., Zahn, R., 1987. Paleoproductivity of oceanic upwelling and the effect on atmospheric CO_2 and climatic change during deglaciation times. In: Berger, W.H., Labeyrie, L.D. (Eds.), Abrupt climatic change: evidence and implications. NATO ASI Series. Series C: Mathematical and Physical Sciences. D. Reidel Publishing Company, Dordrecht, pp. 311–337.

Sarnthein, M., Winn, K., Jung, S.J.A., Duplessy, J.-C., Labeyrie, L., Erlenkeuser, H., Ganssen, G., 1994. Changes in east Atlantic deepwater circulation over the last 30,000 years: eight time slice reconstructions. Paleoceanography 9 (2), 209–267.

Schulz, M., Stattegger, K., 1997. Spectrum: spectral analysis of unevenly spaced paleoclimatic time series. Computers and Geosciences 23, 929–945.

Siedler, G., Onken, R., 1996. Eastern recirculation. In: Krauss, W. (Ed.), The Warmwatersphere of the North Atlantic Ocean. Bornträger, Berlin, pp. 339–364.

Speth, P., Detlefsen, H., Sierts, H.-W., 1978. Meteorological influence on upwelling off Northwest Africa. Deutsche Hydrographische Zeitschrift 31, 95–104.

Strub, P.T., Korso, P.M., Huyer, A., 1991. The nature of the cold filaments in the California Current system. Journal of Geophysical Research 96 (C8), 14743–14768.

Stuiver, M., Braziunas, T.F., 1993. Modelling atmospheric ^{14}C influences and ^{14}C ages of marine samples to 10,000 BC. Radiocarbon 35 (1), 137–189.

Stuiver, M., Reimer, P.J., Bard, E., Beck, J.W., Burr, G.S., Hughen, K.A., Kromer, B., McCormac, F.G., van der Plicht, J., Spurk, M., 1998. INTCAL98 radiocarbon age calibration, 24,000 cal BP. Radiocarbon 40 (3), 1041–1083.

Sweeney, R.E., Kaplan, I.R., 1980. Natural abundances of ^{15}N as a source indicator for near-shore marine sedimentary and dissolved nitrogen. Marine Chemistry 9, 81–94.

Tyson, R.V., 1995. Sedimentary organic matter. Chapman & Hall, London, 615 pp.

Van Camp, L., Nykjær, L., Mittelstaedt, E., Schlittenhardt, P., 1991. Upwelling and boundary circulation off Northwest Africa as depicted by infrared and visible satellite observations. Progress in Oceanography 26, 357–402.

Wagner, T., Dupont, L., 1999. Terrestrial organic matter in marine sediments: analytical approaches and eolian-marine records of the central Equatorial Atlantic. In: Fischer, G., Wefer, G. (Eds.), Use of Proxies in Paleoceanography: Examples from the South Atlantic. Springer, Berlin, Heidelberg, pp. 547–574.

Wefer, G., cruise participants, 1997. Report and preliminary results of Meteor cruise M 37/1, Lisbon-Las Palmas, 04.12.1996–23.12.1996. Berichte, 90. Fachbereich Geowissenschaften, Universität Bremen, Bremen, 79 pp.

Wefer, G., Berger, W.H., Bijma, J., Fischer, G., 1999. Clues to ocean history: a brief overview of proxies. In: Fischer, G., Wefer, G. (Eds.), Use of Proxies in Paleoceanography: Examples from the South Atlantic. Springer, Berlin, Heidelberg, pp. 1–68.